JOURNAL OF VIROLOGY, Oct. 2007, p. 10981–10990 Vol. 81, No. 20
0022-538X/07/$08.00+0 doi:10.1128/JVI.01033-07

The Coronavirus Spike Protein Induces Endoplasmic Reticulum Stress and Upregulation of Intracellular Chemokine mRNA Concentrations[▽]

Gijs A. Versteeg, Paula S. van de Nes, Peter J. Bredenbeek, and Willy J. M. Spaan*

Molecular Virology Laboratory, Department of Medical Microbiology, Center of Infectious Diseases, Leiden University Medical Center, P.O. Box 9600, 2300 RC Leiden, The Netherlands

Received 11 May 2007/Accepted 18 July 2007

Murine hepatitis virus (MHV) and severe acute respiratory syndrome (SARS) coronavirus (CoV) are two of the best-studied representatives of the family *Coronaviridae*. During CoV infection, numerous cytokines and chemokines are induced in vitro and in vivo. Human interleukin 8 and its mouse functional counterpart, CXCL2, are early-expressed chemokines. Here we show that SARS-CoV and MHV induce endoplasmic reticulum (ER) stress and Cxcl2 mRNA transcription during infection in vitro. Expression of the viral spike protein significantly induced ER stress and Cxcl2 mRNA upregulation, while expression of the other structural genes did not. Additional experiments with UV-inactivated virus, cell-cell fusion-blocking antibodies, and an MHV mutant with a defect in spike protein maturation demonstrated that spike-host interactions in the ER are responsible for the induction of ER stress and subsequent Cxcl2 mRNA transcription. Despite significant increases in levels of Cxcl2 mRNA and functional nucleus-to-cytoplasm RNA transport, no CXCL2 protein was released into the medium from MHV-infected cells. Yet Sendai virus-infected cells showed substantial Cxcl2 mRNA induction and a simultaneous increase in levels of secreted CXCL2 protein. Our results demonstrate that expression of CoV spike proteins induces ER stress, which could subsequently trigger innate immune responses. However, at that point in infection, translation of host mRNA is already severely reduced in infected cells, preventing the synthesis of CXCL2 and ER stress proteins despite their increased mRNA concentrations.

Murine hepatitis virus (MHV) is one of the best-studied coronaviruses (CoVs) and serves as a valuable model for other (group 2) CoVs such as severe acute respiratory syndrome (SARS) CoV, the causative agent of the 2003 outbreak of SARS (19, 51). Human CoVs are the second most frequent cause of the common cold. In addition, CoVs cause economically important diseases of cattle, poultry, and pigs. Since the emergence of SARS-CoV, several new human and animal CoVs have been identified, emphasizing the constant occurrence of new, potentially harmful CoVs and the necessity to further investigate their life cycles and interactions with host cells.

The CoV genome consists of single-stranded RNA of positive polarity and encompasses approximately 30,000 nucleotides. CoVs express subgenomic RNAs that encode accessory and structural proteins. The S, M, and E proteins are associated with cellular membranes, while N resides in the cytoplasm. In MHV, the 180-kDa S protein is cleaved by a cellular protease during virus maturation into two subunits that remain noncovalently associated (12, 13, 32). SARS-CoV S is cleaved during viral entry (20, 33). The S protein mediates binding to carcinoembryonic antigen-related adhesion molecule 1 (CEACAM1) and angiotensin-converting enzyme 2 (ACE2), the specific receptors for MHV and SARS-CoV, respectively (16, 34). Accordingly, antibodies against S can neutralize virus infectivity (17). Furthermore, the S protein induces fusion of the viral envelope with host cell membranes and cell-cell fusion (34, 56). Spike proteins are synthesized in the cytoplasm, cotranslationally translocated to the endoplasmic reticulum (ER), and subsequently transported to the Golgi apparatus (56). A fraction of S is eventually transported to the plasma membrane, where it can mediate cell-cell fusion (42, 55).

Viral glycoproteins can induce ER stress during infection as a result of incorrect folding or accumulation in the ER lumen (8, 25). Cells can respond in several ways to reduce the burden imposed by unfolded proteins in the ER, ways that are collectively known as the unfolded-protein response (UPR). Induction of UPR results in transcriptional activation of genes encoding ER-resident molecular chaperones to increase protein-folding activity and repression of protein synthesis. Three distinct branches that orchestrate the UPR have been identified so far (49). Binding to unfolded proteins by ER chaperones results in activation of protein kinase R-like ER kinase (PERK), activating transcription factor 6 (ATF6), and inositol-requiring enzyme 1 (IRE1). IRE1 mediates the splicing of mRNA encoding the transcription factor X box-binding protein 1 (XBP1), leading to a frame shift and subsequent translation of functional XBP1 protein (60). The active transcription factor XBP1 (XBP1s) can in turn stimulate different subsets of genes encoding proteins that promote the folding, transport, and degradation of ER proteins. The IRE1/XBP1- and ATF6-dependent branches are specific for ER stress, while the PERK-dependent pathway is shared with other cellular stress responses (38). Expression of the ER-resident protein Herpud1 is regulated by both the ER stress-specific and the shared branches of the UPR (38). Herpud1 balances folding capacity and protein loads in the ER and also plays a role in stabilizing cellular Ca^{2+} homeostasis (9, 28). Expression of

* Corresponding author. Mailing address: Molecular Virology Laboratory, Department of Medical Microbiology, Leiden University Medical Center, LUMC E4-P, P.O. Box 9600, 2300 RC Leiden, The Netherlands. Phone: 31715261652. Fax: 31715261667. E-mail: w.j.m.spaan@lumc.nl.

▽ Published ahead of print on 1 August 2007.

Herpud1 is strongly induced by ER stress and can be considered a hallmark of ER stress (28). ER stress can also induce the expression of innate immunity molecules such as chemokines (22, 61). Chemokines are excreted by infected cells and attract specialized immune cells to sites of infection. Recent microarray analysis of MHV-infected cells showed induction of several ER stress markers, including Herpud1, and several chemokines, including Cxcl2 (58). Mouse CXCL2 is a functional counterpart of human interleukin 8 and has been associated with the recruitment of inflammatory cells during various diseases (18, 24, 46, 54). During MHV infection in vivo, CXCL2 mediates antiviral responses, but it has also been implicated in the development of immunopathology (46, 47). Cells carry out steady-state production of CXCL2 from basal levels of Cxcl2 mRNA, since it is also involved in other cellular processes. The clear coregulation of ER stress genes and chemokine genes during microarray analysis suggested that MHV infection activates ER stress pathways that in turn induce innate immune responses. In addition, it has been shown that the SARS-CoV spike protein induces ER stress and activation of PERK (8). However, the ATF6 and IRE1 branches were not activated. The authors concluded that SARS-CoV S protein specifically modulates the UPR to facilitate viral replication.

In this study we show that the MHV spike protein, like that of SARS-CoV, induces ER stress. MHV infection resulted in extensive expression of UPR markers such as Herpud1 and XBP1s, while SARS-CoV infection upregulated only a limited set of UPR genes. Both viruses potently induced Cxcl2 mRNA expression during infection in vitro. Despite the significant increase in the Cxcl2 mRNA concentration, no CXCL2 protein could be detected in the cytoplasm or medium of infected cells. From the data we concluded that CoV infection induces ER stress and triggers the innate immune system. However, at that point, translation of these cellular mRNAs is already severely reduced, resulting in no significant CXCL2 or HERPUD1 protein synthesis in infected cells, despite their increased mRNA concentrations.

MATERIALS AND METHODS

Cells, viruses, and plaque assay. Mouse L cells and Sac$^-$ cells were cultured and infected with MHV and MHV temperature-sensitive (*ts*) mutants as described previously (29, 30). Strain A59 of MHV was obtained from ATCC. SARS-CoV strain Frankfurt 1 was grown on Vero E6 cells, and all work with infectious SARS-CoV was performed as described previously (52). A T7 RNA polymerase-expressing recombinant vaccinia virus (vTF7.3) stock was propagated on RK13 cells (21). Recombinant Sendai virus H4 (SeV-H4) was kindly provided by D. Kolakofsky (6). MHV and vTF7.3 titers were determined by plaque assays on L cells, while SARS-CoV was quantified by plaque assays on L cells stably expressing ACE2 (L-ACE2) (57).

Protein expression and immunoprecipitation. Mouse L cells were infected with recombinant vaccinia virus (vTF7.3) at a multiplicity of infection (MOI) of 10. At 1 h postinfection (p.i.), cells were transfected with 4 μg of pTUM-M (42), pTUM-N (56), pTUM-S (5), or pIRES-E (5) DNA using Lipofectamine 2000 (Invitrogen) as recommended by the manufacturer. Cells were metabolically labeled with [^{35}S]methionine-cysteine (^{35}S Redivue Promix; Amersham Pharmacia) in a medium lacking methionine and cysteine from 5 to 8 h posttransfection. Cells were lysed, further processed for immunoprecipitation with rabbit sera recognizing MHV S, E, M, and N (4, 48) or HERPUD1 (50), and analyzed by sodium dodecyl sulfate (SDS)-polyacrylamide gel electrophoresis (3).

Viral infection and RNA isolation and RT-qPCR. L or L-ACE2 cells were seeded in 35-mm-diameter dishes and infected with MHV-A59 or SARS-CoV at an MOI of 10 (58). SeV-H4 infections were carried out in complete medium for 30 to 45 min at 37°C, after which complete medium was added to the inoculum. The medium was harvested for virus titration at the indicated time points. Total RNA was isolated from the cells using TRIzol reagent (Invitrogen) as recommended by the manufacturer. Cytoplasmic and nuclear RNAs were isolated by RNeasy (QIAGEN) as previously described (45). Isolated RNA was treated with 2 U of DNase I (Invitrogen) at 37°C for 30 min to remove potential genomic DNA contamination. Reverse transcription-quantitative PCR (RT-qPCR) was performed as described previously (58). In brief, cDNA was synthesized from total cellular RNA using random hexamers and was used for RT-qPCR with gene-specific primers. (Nucleotide sequences are available upon request.) qPCR was performed using Amplitaq Gold polymerase (Applied Biosystems) and SYBR Green I (Molecular Probes). The amount of RNA was determined with respect to standardized samples and expressed in relative units. The results of quantification were normalized to the amount of glyceraldehyde-3-phosphate dehydrogenase (GAPDH) mRNA in the same sample. Each qPCR was performed in triplicate, and means and standard deviations were calculated.

Xbp1 mRNA splicing assay. Xbp1 mRNA splicing was assayed as described previously (7). In brief, Xbp1 was first PCR amplified from randomly primed cDNA using primers mXBP1.3S (5′ A AAC AGA GTA GCA GCG CAG ACT GC 3′) and mXBP1.12AS* (5′ TC CTT CTG GGT AGA CCT CTG GGA G 3′) and then analyzed on a 2% native agarose gel.

Immunofluorescence assay. Cells were seeded on glass coverslips in 35-mm-diameter wells and infected and transfected as described above. Coverslips were removed at set intervals and fixed in 3% paraformaldehyde. Cells were permeabilized in 0.1% Triton X-100 for 10 min, washed several times in phosphate-buffered saline (PBS) supplemented with 10 mM glycine, reacted with 1:1,000-diluted antibody k134 (48), and developed with a Cy3-conjugated 1:2,000-diluted donkey anti-rabbit antibody (Jackson Immunoresearch Laboratories).

Neutralization of viral infectivity by k134 serum. One-tenth volume of polyclonal antibody k134 (48) was added to the medium of MHV-A59-infected L cells at 3 h p.i., and cells were further incubated until harvesting. At 8.5 h p.i., RNA was isolated and cells were fixed for the immunofluorescence assay.

Virus binding assay. To prepare [^{35}S]-labeled MHV-A59, L cells were infected with MHV-A59 (MOI, 5) and radioactively labeled with 100 μCi/ml [^{35}S]methionine-cysteine from 5 to 8 h p.i. The supernatant containing radiolabeled virions was harvested at 8 h p.i. and clarified by centrifugation at 4,000 rpm for 10 min in the cold. Virions were loaded onto a 20% sucrose cushion in HES buffer (20 mM HEPES, 1 mM EDTA, 100 mM NaCl [pH 6.7]), followed by ultracentrifugation in a Beckman SW32 rotor at 25,000 rpm for 4 h. The pellet was dissolved in HES buffer (pH 6.7). A part of the preparation was exposed to increasing amounts of UV-irradiation for subsequent binding and entry studies. UV-irradiated virus has been used and published before as an accepted method for the study of CoV entry (15, 36). Also, data from other viruses indicate that entry still occurs after careful UV irradiation of the virus preparation (40). Great care was taken to UV irradiate our preparation in the shortest time possible so as to avoid affecting the spike proteins. Virus titers of the samples from the various exposure times were determined by plaque assay. The inactivated virus batch with the shortest UV exposure time yielding no detectable infectious virus was used for binding assays. L cells in 35-mm-diameter dishes were washed twice with ice-cold PBS-DEAE and incubated with UV-irradiated or nonirradiated radiolabeled virions (MOI, 20) on ice at 4°C for 1 h. Cells were washed three times with ice-cold PBS-DEAE and subsequently incubated at 37°C for an additional 8 h with Dulbecco's modified Eagle medium–3% fetal calf serum or lysed with PBS containing 1% SDS. Radioactivity was quantified in a liquid scintillation counter (LS 6500; Beckman Coulter).

ELISA. CXCL2 protein concentrations were determined in 50 μl of 0.5% NP-40 (vol/vol)-treated cell culture supernatant using the MIP-2 DuoSet enzyme-linked immunosorbent assay (ELISA) development kit (R&D Systems, Minneapolis, MN) as recommended by the manufacturer. Optical density was determined with a multichannel spectrophotometer (Titertek Multiskan MCC/340; Labsystem) at 450 nm. Wavelength correction was set at 540 nm. Twofold serial dilutions of the DuoSet recombinant mouse Cxcl2 standard were used to build six point standard curves.

RESULTS

Chemokine Cxcl2 expression is induced upon MHV or SARS-CoV infection. To study chemokine induction during CoV infection in more detail, L cells were infected with MHV at a high MOI. Intracellular Cxcl2 mRNA concentrations were determined by RT-qPCR. Cxcl2 mRNA levels started to increase between 5 and 6 h p.i., approximately 1 h after virus release into the medium was detected, reaching 40-fold induc-

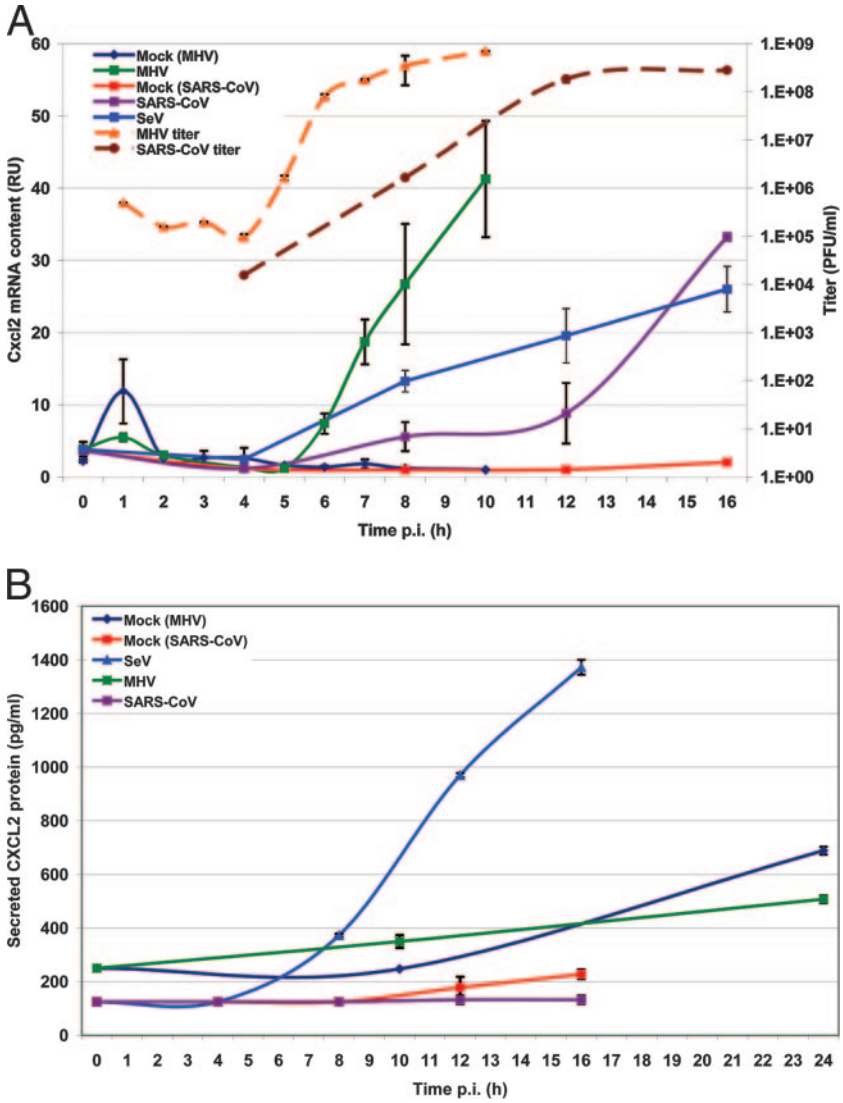

FIG. 1. MHV and SARS-CoV induce Cxcl2 mRNA expression but prevent CXCL2 protein synthesis. L cells were infected with MHV, or L-ACE2 cells were infected with SARS-CoV, at an MOI of 10. (A) Release of infectious MHV was determined by a plaque assay, and isolated total RNA was analyzed for Cxcl2 expression by RT-qPCR. Values were normalized to GAPDH and expressed as induction (*n*-fold). RU, relative units. (B) Supernatants from MHV-infected L cells and SARS-CoV-infected L-ACE2 cells were analyzed for protein production by a CXCL2-specific ELISA. SeV infection was used as a positive control.

tion compared to mock-infected cells at 10 h p.i. (Fig. 1A). To allow for a comparison of MHV with SARS-CoV infection, L-ACE2 cells were infected. In these cells, SARS-CoV completed one replication cycle, with kinetics similar to those in Vero E6 cells, in approximately 12 h. SARS-CoV-infected L-ACE2 cells showed Cxcl2 upregulation comparable to that for MHV infection, although with slower kinetics (Fig. 1A). Cxcl2 upregulation started between 4 and 8 h p.i. and was increased more than 30-fold at 16 h p.i. At 16 h p.i., SARS-CoV-infected cells displayed a severe cytopathic effect (CPE), which prevented further measurements.

To investigate whether the increased Cxcl2 mRNA concentration was also reflected in secreted CXCL2 protein, concentrations of CXCL2 in supernatants of infected cells were determined by ELISA. Surprisingly, very little CXCL2 was detected in the medium of infected cells within the first 24 h after MHV infection (Fig. 1B). Persistent CoV infections can be readily established in vitro. After an initial cytolytic infection, virus-carrier cultures arise in which a fraction of the cells produce infectious virus for extended periods (27, 31). Even when the time of infection was extended to 96 h by using an MHV carrier culture with highly elevated levels of Cxcl2 mRNA (260-fold), no secreted CXCL2 protein was detectable (data not shown). SARS-CoV-infected cells also produced no CXCL2 despite significant Cxcl2 mRNA induction (Fig. 1B). CXCL2 protein concentrations in cell lysates also did not increase (data not shown), suggesting an effect of MHV infection on translation rather than protein export. To control for CXCL2 protein production and secretion, L-ACE2 cells were infected with SeV. SeV-infected L-ACE2 cells showed substantial Cxcl2 mRNA induction and a simultaneous increase in the level of secreted CXCL2 protein (Fig. 1A and B).

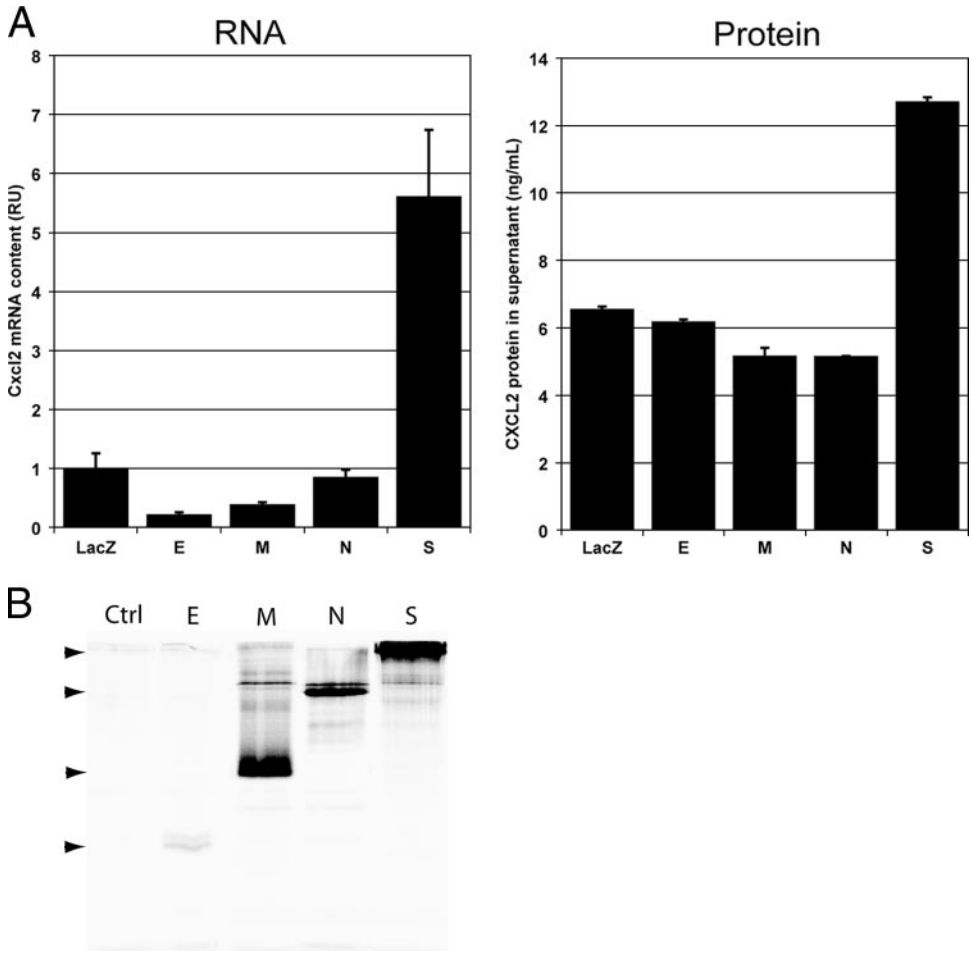

FIG. 2. MHV spike protein induces Cxcl2 mRNA and protein expression. MHV structural genes were transiently expressed in L cells by using a vaccinia virus T7 polymerase system. (A) Cxcl2 mRNA concentrations were determined by RT-qPCR, and CXCL2 protein concentrations in the supernatant were analyzed by ELISA. RU, relative units. (B) Proteins were metabolically labeled, and expression of viral proteins was determined by immunoprecipitation with MHV-specific antibodies and analysis by SDS-polyacrylamide gel electrophoresis. Ctrl, control.

Expression of MHV spike protein results in Cxcl2 induction. To determine if MHV structural proteins were involved in the induction of Cxcl2, S, E, M, and N were ectopically expressed using vaccinia virus vTF7.3. At 6 h after transfection of the plasmids for the individual expression of the MHV structural genes, Cxcl2 mRNA levels were determined. Vaccinia virus-induced CPE prevented analysis at later time points. Specific immunoprecipitations were performed to confirm the expression of all structural genes. Despite the obvious expression of MHV E, M, and N (Fig. 2B), no significant increase in the levels of Cxcl2 mRNA was observed, while expression of S increased Cxcl2 levels 5.5-fold (Fig. 2A). In order to determine if increased Cxcl2 mRNA was translated, CXCL2 concentrations in the medium of transfected cells were determined by a specific ELISA. In contrast to the results for MHV-infected cells, the MHV S protein-induced increase in Cxcl2 mRNA levels resulted in a reproducible twofold increase in CXCL2 concentrations in the medium of cells with vaccinia virus vTF7.3-driven expression of MHV S (Fig. 2A). Since CoV spike proteins fulfill multiple functional interactions during infection, we next set out to identify spike-host interactions triggering chemokine expression.

Cxcl2 induction is independent of MHV-cell binding. Virus particles were radioactively labeled in order to determine the efficiency of binding. To determine whether virus attachment to the host cells is the trigger for Cxcl2 increase, L cells were incubated on ice with a preparation of UV-irradiated MHV that could still bind to cells but could not initiate replication. A nonirradiated virus stock was used as a control. After incubation on ice that allowed virus binding but not entry, unbound virus was carefully removed. Subsequently, radioactivity was determined as a measure of virus binding to ensure equal binding of irradiated and nonirradiated virus preparations. Parallel samples were washed and shifted from ice to incubation at 37°C. At 8.5 h p.i., total RNA was isolated and Cxcl2 mRNA concentrations were determined. Cell binding was similar for both infectious and UV-inactivated viruses (Fig. 3A). However, only infection with infectious MHV resulted in a 20-fold increase in Cxcl2 mRNA levels; incubation with UV-inactivated virus did not increase Cxcl2 mRNA levels above

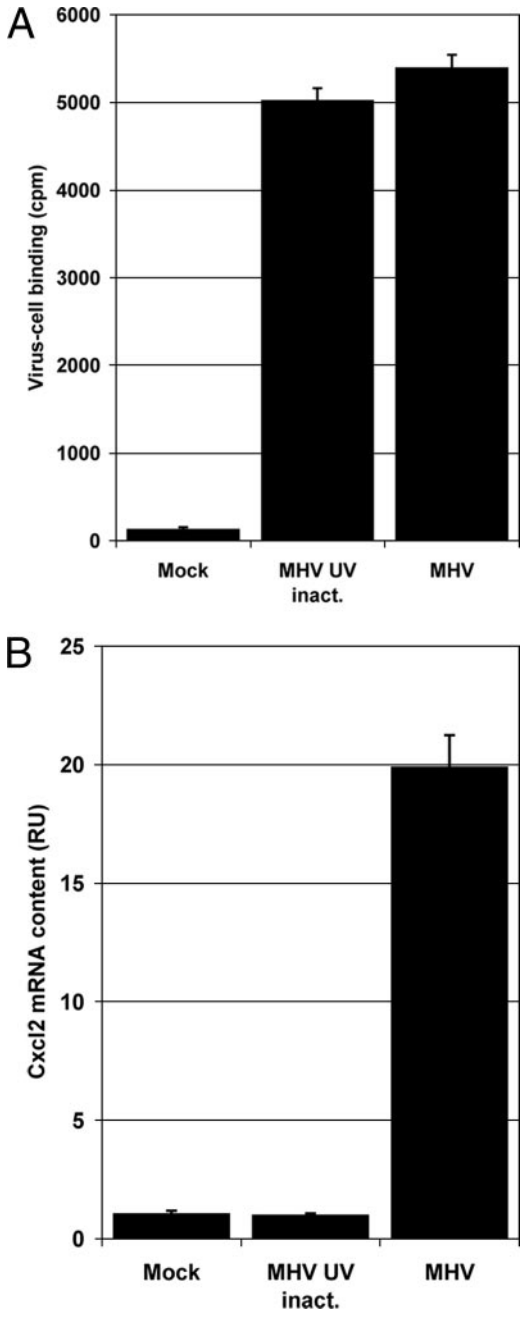

FIG. 3. MHV-cell binding is not required for Cxcl2 induction. L cells were incubated on ice with radioactively labeled MHV or an equivalent amount of UV-inactivated (inact.) MHV. (A) After extensive removal of unbound virus, radioactivity was determined as a measure of virus binding. (B) Parallel samples were further incubated at 37°C. At 8.5 h p.i., total RNA was harvested and Cxcl2 mRNA concentrations were determined by RT-qPCR. RU, relative units.

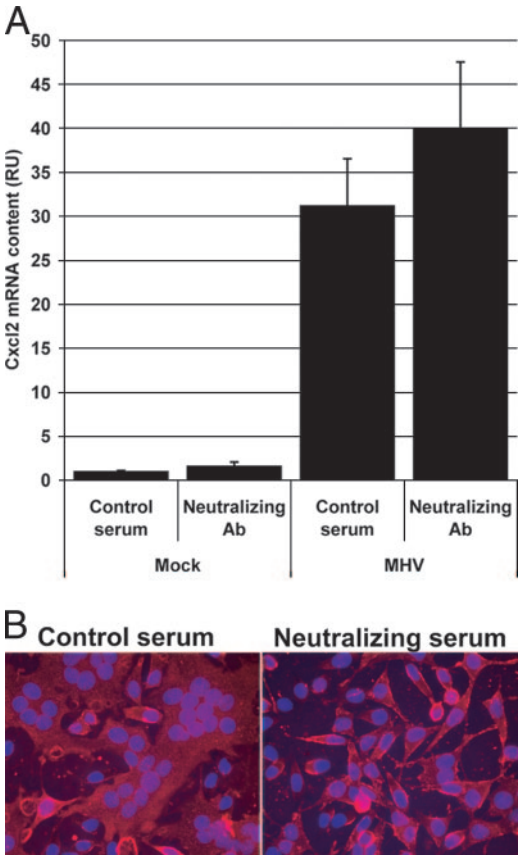

FIG. 4. Syncytium formation and progeny virus-cell binding are not involved in Cxcl2 induction during MHV infection. L cells were infected with MHV. At 3 h p.i., virus binding and syncytium formation were blocked by addition of neutralizing antibodies (Ab) or a control serum from nonimmunized rabbits to the medium. At 8.5 h p.i., the Cxcl2 mRNA concentration was determined by RT-qPCR (A) and cell-cell fusion was assessed by MHV-specific immunofluorescence microscopy (B). RU, relative units.

those found in mock-infected cells (Fig. 3B), demonstrating that MHV binding and subsequent internalization do not result in Cxcl2 induction.

Syncytium formation and progeny virus binding are not required for Cxcl2 induction. Cxcl2 induction coincides with the start of cell-cell fusion and the potential binding of released progeny virus to the infected cells. To determine their involvement in Cxcl2 induction, the binding of newly produced virions to the cell surface and the formation of syncytia were blocked in MHV-infected cells by addition of neutralizing antibodies to the medium. At the concentration used, the antibodies completely neutralized all infectious virus (data not shown) and prevented cell-cell fusion (Fig. 4B). Antibody treatment by itself did not increase Cxcl2 mRNA levels in mock-infected cells. Nevertheless, Cxcl2 was induced to similar degrees in cells treated with neutralizing serum and those treated with control serum (30- to 40-fold [Fig. 4A]). These data show that neither CoV spike-induced cell-cell fusion nor the binding of newly produced virus to the cells is responsible for the observed increase in Cxcl2 levels during MHV infection.

Cxcl2 induction during MHV infection is initiated by spike interactions in the ER. Since intracellular spike-host interactions were likely to underlie Cxcl2 induction, we set out to study the maturation and localization requirements of the spike protein for Cxcl2 induction. Cells were infected with wild-type MHV or a *ts* mutant virus (*ts*379) encoding a spike protein that is retained in the ER at the restrictive temperature

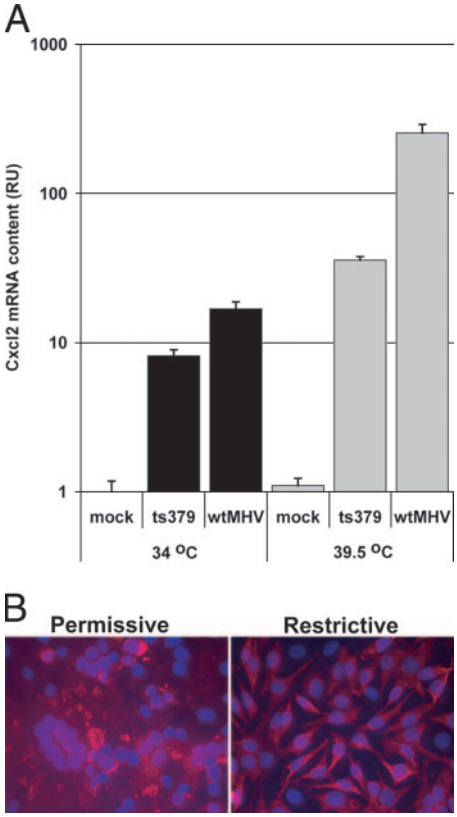

FIG. 5. Cxcl2 induction during MHV infection is initiated by spike interactions in the ER. L cells were infected at the permissive temperature with wild-type (wt) MHV or *ts*379, the spike protein of which is retained in the ER at the restrictive temperature. (A) After incubation for 16 h at the permissive (34°C) or 8.5 h at the restrictive (39.5°C) temperature, Cxcl2 concentrations were determined by RT-qPCR. RU, relative units. (B) Lack of cell-cell fusion as a control for abolished spike maturation during *ts*379 infection at the restrictive temperature was confirmed by MHV-specific immunofluorescence microscopy.

as a result of impaired oligomerization (37). After incubation for 16 h at the permissive temperature (34°C) or 8.5 h at the restrictive temperature (39.5°C), Cxcl2 mRNA concentrations were determined. Wild-type MHV spike expression resulted in the formation of syncytia at both the permissive and the restrictive temperature. *ts*379 spikes induced cell-cell fusion only at the permissive temperature, not at the restrictive (Fig. 5B), confirming the absence of correct spike maturation and cell surface expression in *ts* mutant-infected cells. Both wild-type MHV and *ts*379 infection resulted in substantial increases in cellular Cxcl2 mRNA concentrations irrespective of the maturation of the MHV S protein (Fig. 5A). At both temperatures, induction by the *ts*379 spike was lower than that by the wild-type spike. Overall, these data suggest that spike-host interactions in the ER contribute to Cxcl2 induction, yet viral factors other than the spike may also be partially responsible.

ER stress responses are induced in CoV-infected cells. Since viral glycoproteins can upregulate ER stress-mediated cytokine expression, we determined if the ER stress marker Herpud1 was upregulated in MHV-infected cells. RNA was isolated from MHV-infected cells at various time points and analyzed for Herpud1 expression. As with Cxcl2, Herpud1 induction started between 5 and 6 h p.i. and increased in a linear fashion to 80-fold upregulation at 10 h p.i. (Fig. 6A). As with Cxcl2, immunoprecipitation revealed no increase in HERPUD1 protein concentrations in MHV-infected cells, while treatment with the ER stress inducer tunicamycin increased the synthesis of HERPUD1 (data not shown). Activation of ER stress was also addressed by determining the splicing of ER stress-induced transcription factor Xbp1 mRNA (7). In mock-infected cells and MHV-infected cells at 4 h p.i., predominantly unspliced Xbp1 mRNA was recovered, demonstrating the absence of significant ER stress (Fig. 6B). However, at 8 h p.i., the spliced Xbp1 mRNA variant was predominantly detected in MHV-infected cells, confirming ER stress induction (Fig. 6B). Like MHV infection, SARS-CoV infection induced Herpud1 (25-fold at 16 h p.i.) with kinetics very similar to Cxcl2 upregulation (Fig. 6A). However, no increase in Xbp1 mRNA splicing was observed in SARS-CoV-infected cells. This indicates that differences in UPR activation exist between MHV and SARS-CoV and that some UPR branches are not significantly activated by SARS-CoV. At 16 h p.i., SARS-CoV-infected cells displayed severe CPE, which prevented further measurements. Since ER stress coincided with Cxcl2 induction in CoV-infected cells, we next investigated if MHV spike could specifically induce ER stress, as it did for Cxcl2. MHV structural proteins were expressed, and Herpud1 expression and Xbp1 mRNA splicing were determined. As with Cxcl2, only spike expression upregulated Herpud1 (30-fold [Fig. 7A]) and induced Xbp1 splicing (Fig. 7B). This further substantiates the hypothesis that ER stress could be involved in Cxcl2 induction.

The absence of protein synthesis does not result from disturbed mRNA export from the nucleus. Cxcl2 mRNA upregulation was so far measured in total-RNA extracts. Viral interference with nuclear export of RNA could be the underlying reason for the lack of translation of the elevated levels of Cxcl2 mRNA in infected cells. To further investigate this possibility, cytoplasmic, nuclear, and total RNAs were isolated from MHV-infected cells at 7 h p.i. and compared to RNAs from mock infections. For the three fractions, Cxcl2 mRNA concentrations were determined by RT-qPCR and normalized to GAPDH mRNA levels. No PCR products were recovered from control reactions in which the reverse transcription step was omitted (data not shown). Cxcl2 mRNA was not induced in any of the fractions from mock-infected cells (Fig. 8). However, MHV infection stimulated Cxcl2 production in all fractions investigated: 8.7-fold in total RNA, 13.5-fold in cytoplasmic RNA, and 12.1-fold in nuclear RNA (Fig. 8). Despite some intersample variation, the data clearly show that the Cxcl2 mRNA levels are comparably increased in cytoplasmic and nuclear RNA fractions. This indicates that Cxcl2 mRNA transport from the nucleus is intact and is unlikely the reason for the absence of CXCL2 protein synthesis in MHV-infected cells.

DISCUSSION

In this study, it is demonstrated that lytic MHV and SARS-CoV infection can induce ER stress responses and Cxcl2 mRNA induction. We hypothesize that CoV spike protein-mediated ER stress can initiate the transcription of chemokine genes based on the following observations: (i) MHV and

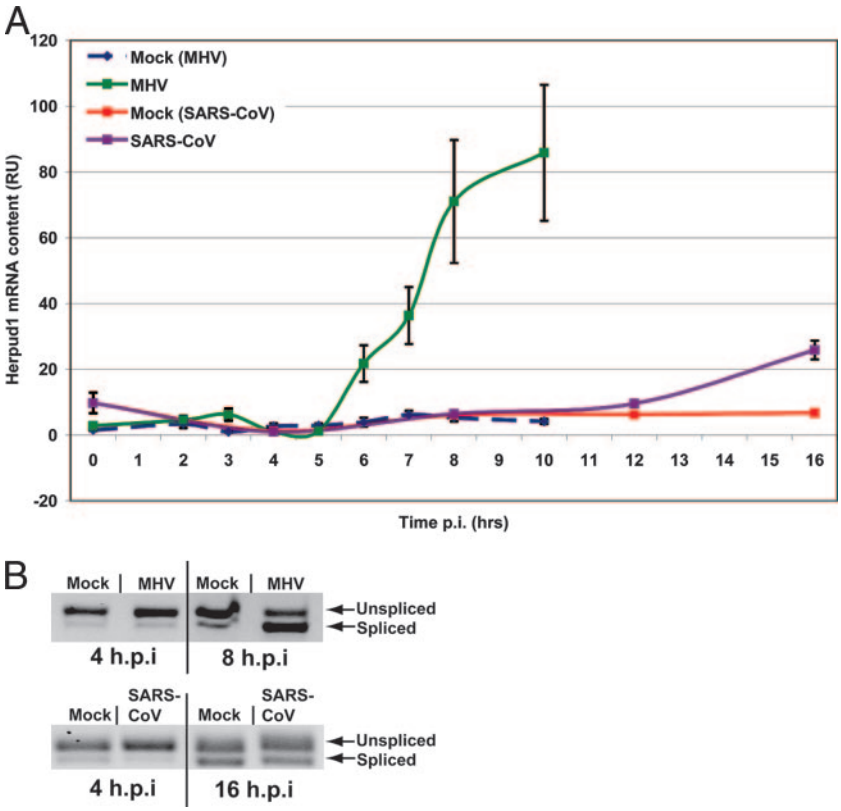

FIG. 6. MHV infection and SARS-CoV infection induce ER stress. (A) L cells were infected with MHV, or L-ACE2 cells were infected with SARS-CoV, at an MOI of 10. Total RNA was analyzed for Herpud1 expression by RT-qPCR. Values were GAPDH normalized and expressed as induction (*n*-fold). RU, relative units. (B) The same samples were analyzed for Xbp1 mRNA splicing during MHV (top) or SARS-CoV (bottom) infection by specific PCR and 2% agarose gel electrophoresis.

SARS-CoV induced ER stress and upregulated chemokine mRNA levels during infection; (ii) ER stress and chemokine mRNA upregulation were both induced only by spike expression, and their expression occurred simultaneously; (iii) ER-retained MHV spike was sufficient to induce Cxcl2 transcription.

The data reported indicate for the first time that in addition to the innate immune sensors that have been described so far, the overload of the ER with viral glycoproteins could also mediate induction of innate immune responses such as transcriptional activation of chemokine genes. Moreover, our data demonstrate that in productively infected cells, CoV-induced translational attenuation contributes to viral evasion of potentially harmful host proteins, such as chemokines. A comparable situation has been described for foot-and-mouth disease virus infection, where type I interferon mRNA is upregulated during infection, but eventually interferon protein production from the increased mRNA levels is prevented (11).

The data presented here indicate two possibilities for the induction of Cxcl2. The first possibility assumes that spike-induced ER stress triggers Cxcl2 induction. The second assumes that spike induces ER stress and Cxcl2 independently of each other. Although a direct link between Cxcl2 induction and ER stress has not been demonstrated in this study, their simultaneous expression and spike dependence, as well as previous reports showing that ER stress can be involved in the induction of innate immunity (22, 61), favor the first model and suggest a link between ER stress and Cxcl2 induction. In support of this, induction of a UPR by tunicamycin also led to Cxcl2 induction (data not shown).

Although our data firmly established the potential of spike accumulation to induce ER stress, other factors during infection could contribute as well. For example, some CoVs assemble their replication complexes on ER membranes and severely limit the size of the ER, thereby making it vulnerable to stress induction (23). The development of a CoV deletion mutant lacking the S gene will be required to address the proportional contributions of S accumulation to activation of a UPR and Cxcl2 transcription in more detail. Several viral glycoproteins, such as influenza A virus hemagglutinin, hepatitis B virus MHBst, simian virus 5 HE, and adenovirus E3/19K, can specifically induce ER stress and activate innate immunity during infection (39, 43, 44, 59). Viruses may benefit from UPR induction, since protein chaperones produced in response to ER stress may aid in the folding of viral proteins, while on the other hand, viral proteins could be degraded as a result of the UPR. Several viruses induce only a subset of the UPR branches and are thought to actively modulate particular parts of the UPR so as to regulate it for their own benefit (62).

Upregulation of Herpud1 mRNA concentrations and Xbp1 splicing during MHV infection (Fig. 6A and B) indicated induction of the IRE1 pathway. SARS-CoV, on the other hand,

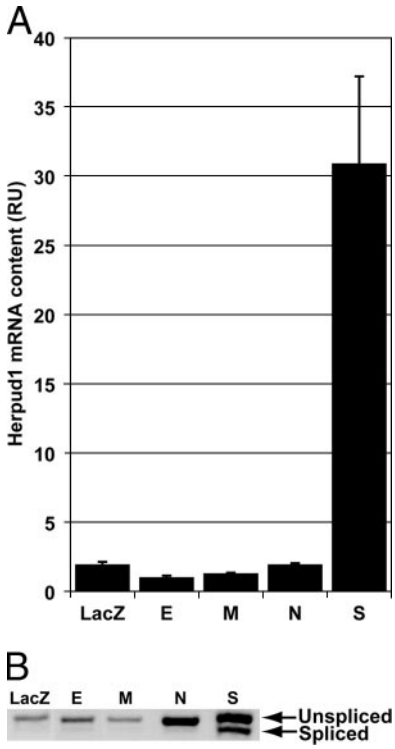

FIG. 7. MHV spike protein induces Herpud1 mRNA. MHV structural genes were transiently expressed in L cells using a vaccinia virus T7 polymerase system. (A) Herpud1 mRNA concentrations were determined by RT-qPCR. RU, relative units. (B) The same samples were analyzed for Xbp1 mRNA splicing by specific PCR and 2% agarose gel electrophoresis.

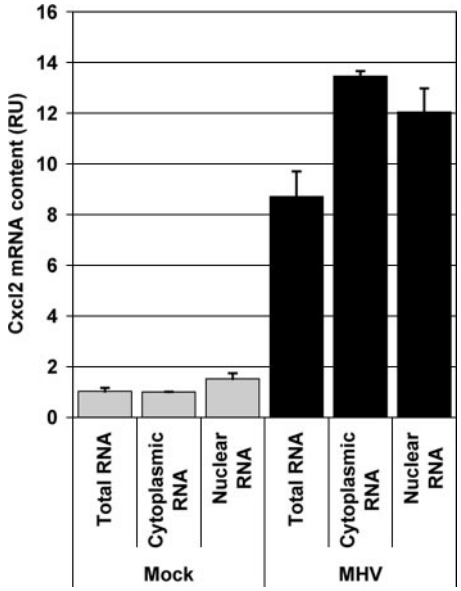

FIG. 8. The absence of protein synthesis does not result from disturbed mRNA export from the nucleus. L cells were infected with MHV at an MOI of 10. Total, cytoplasmic, and nuclear RNAs were isolated at 7 h p.i. and analyzed for Cxcl2 expression by RT-qPCR. Values were GAPDH normalized and expressed as induction (*n*-fold). RU, relative units.

upregulated Herpud1 mRNA concentrations to a lesser extent than MHV (Fig. 6A) and did not induce significant Xbp1 splicing (Fig. 6B). These results are consistent with the recent observation that SARS-CoV spike induced a UPR in 293 cells without Xbp1 mRNA splicing or ATF6 transcriptional activity (8). These findings indicate that SARS-CoV spike expression induces only a limited set of UPR pathways. This implies that SARS-CoV could suppress certain ER stress regulators, as has been shown for hepatitis C virus (62). Alternatively, the differences may also be explained by the fact that MHV has a shorter life cycle, due to which it imposes more-strenuous conditions on infected cells than SARS-CoV, since viral proteins are synthesized in a shorter time span.

Activation of PERK, ATF-6, and IRE-1 occurs at a post-translational level and can directly initiate other cellular responses that do not require protein synthesis for their activation, such as p38 mitogen-activated protein kinase (MAPK) (35, 53). Both SARS-CoV and MHV induce p38 MAPK, the activation of which stimulates virus replication, progeny virus production, and the onset of CPE (1, 41). One could hypothesize that the UPR activates cellular pathways, such as p38 MAPK, that have a positive effect on the viral life cycle. Indeed, preliminary experiments using a specific p38 inhibitor showed a significant reduction in the level of MHV production during in vitro infection (G. A. Versteeg et al., unpublished data).

Experimental results addressing the significance of viral UPR induction in vivo remain scarce. So far, induction of ER stress and its influence on pathogenicity in vivo have been shown only during infection with a neurovirulent retrovirus (14). Infection with a virulent virus strain was accompanied by ER stress marker upregulation in the brain, whereas expression of those markers was absent in mice infected with an avirulent strain (14). The MHV spike protein has been implicated in (neuro)virulence as well (47), and it will be interesting to investigate whether differences in ER stress induction may also be involved there.

Both the MHV and the SARS-CoV spike protein are sufficient to induce a UPR and CXC-type chemokine upregulation (this work; see also reference 10). Yet spike proteins can already be detected at 2 to 3 h before the induction of these cellular responses. Therefore, we propose that it is not mere S expression that triggers the induction but rather the accumulation of S protein in the ER. Expression of *ts*379 spike induced substantial amounts of Cxcl2 mRNA, yet always less than those induced by wild-type MHV spike (Fig. 5A). The spike expression levels of the *ts*379 mutant are lower than those of the wild-type virus (37). This is true at both the permissive and the restrictive temperature, although the difference from the wild type is most extensive at the restrictive temperature. These results correlate with the observations presented in Fig. 5A and may explain the differences observed in Cxcl2 mRNA upregulation. Very low leakiness and reversion frequency (30) and an absence of syncytia at the restrictive temperature (Fig. 5B) make the involvement of leaky spike maturation in Cxcl2 induction highly unlikely.

During productive MHV infection in vitro, total protein synthesis drops steeply around 6 h p.i. (O. Slobodskaya and W. J. M. Spaan, unpublished data), while Cxcl2 and Herpud1

mRNA induction starts at that time. This could well explain the absence of translation of the upregulated Cxcl2 and Herpud1 mRNAs. In contrast to infection, ectopic spike expression induced CXCL2 protein, indicating that viral factors other than spike are responsible for the lack of CXCL2 protein production in infected cells. The lack of secreted CXCL2 protein in the medium of SARS-CoV-infected cells, despite a significant increase in mRNA levels, suggests that similar translational inhibition could occur during SARS-CoV infection as during MHV infection. These data suggest that attenuation of cellular translation might be a general feature of productively CoV infected cells and a strategy to prevent cellular synthesis of antiviral proteins.

ACKNOWLEDGMENT

This work was supported by EU grant FP6 SARS-DTV Network (SP22-CT-2004-511064).

REFERENCES

1. **Banerjee, S., K. Narayanan, T. Mizutani, and S. Makino.** 2002. Murine coronavirus replication-induced p38 mitogen-activated protein kinase activation promotes interleukin-6 production and virus replication in cultured cells. J. Virol. **76:**5937–5948.
2. **Bensaude, E., J. L. Turner, P. R. Wakeley, D. A. Sweetman, C. Pardieu, T. W. Drew, T. Wileman, and P. P. Powell.** 2004. Classical swine fever virus induces proinflammatory cytokines and tissue factor expression and inhibits apoptosis and interferon synthesis during the establishment of long-term infection of porcine vascular endothelial cells. J. Gen. Virol. **85:**1029–1037.
3. **Bos, E. C., L. Heijnen, W. Luytjes, and W. J. Spaan.** 1995. Mutational analysis of the murine coronavirus spike protein: effect on cell-to-cell fusion. Virology **214:**453–463.
4. **Bos, E. C., W. Luytjes, and W. J. Spaan.** 1997. The function of the spike protein of mouse hepatitis virus strain A59 can be studied on virus-like particles: cleavage is not required for infectivity. J. Virol. **71:**9427–9433.
5. **Bos, E. C., W. Luytjes, H. V. van der Meulen, H. K. Koerten, and W. J. Spaan.** 1996. The production of recombinant infectious DI-particles of a murine coronavirus in the absence of helper virus. Virology **218:**52–60.
6. **Cadd, T., D. Garcin, C. Tapparel, M. Itoh, M. Homma, L. Roux, J. Curran, and D. Kolakofsky.** 1996. The Sendai paramyxovirus accessory C proteins inhibit viral genome amplification in a promoter-specific fashion. J. Virol. **70:**5067–5074.
7. **Calfon, M., H. Zeng, F. Urano, J. H. Till, S. R. Hubbard, H. P. Harding, S. G. Clark, and D. Ron.** 2002. IRE1 couples endoplasmic reticulum load to secretory capacity by processing the XBP-1 mRNA. Nature **415:**92–96.
8. **Chan, C. P., K. L. Siu, K. T. Chin, K. Y. Yuen, B. Zheng, and D. Y. Jin.** 2006. Modulation of the unfolded protein response by the severe acute respiratory syndrome coronavirus spike protein. J. Virol. **80:**9279–9287.
9. **Chan, S. L., W. Fu, P. Zhang, A. Cheng, J. Lee, K. Kokame, and M. P. Mattson.** 2004. Herp stabilizes neuronal Ca^{2+} homeostasis and mitochondrial function during endoplasmic reticulum stress. J. Biol. Chem. **279:**28733–28743.
10. **Chang, Y. J., C. Y. Liu, B. L. Chiang, Y. C. Chao, and C. C. Chen.** 2004. Induction of IL-8 release in lung cells via activator protein-1 by recombinant baculovirus displaying severe acute respiratory syndrome-coronavirus spike proteins: identification of two functional regions. J. Immunol. **173:**7602–7614.
11. **Chinsangaram, J., M. E. Piccone, and M. J. Grubman.** 1999. Ability of foot-and-mouth disease virus to form plaques in cell culture is associated with suppression of alpha/beta interferon. J. Virol. **73:**9891–9898.
12. **de Haan, C. A., K. Stadler, G. J. Godeke, B. J. Bosch, and P. J. Rottier.** 2004. Cleavage inhibition of the murine coronavirus spike protein by a furin-like enzyme affects cell-cell but not virus-cell fusion. J. Virol. **78:**6048–6054.
13. **Delmas, B., and H. Laude.** 1990. Assembly of coronavirus spike protein into trimers and its role in epitope expression. J. Virol. **64:**5367–5375.
14. **Dimcheff, D. E., M. A. Faasse, F. J. McAtee, and J. L. Portis.** 2004. Endoplasmic reticulum (ER) stress induced by a neurovirulent mouse retrovirus is associated with prolonged BiP binding and retention of a viral protein in the ER. J. Biol. Chem. **279:**33782–33790.
15. **Dove, B., G. Brooks, K. Bicknell, T. Wurm, and J. A. Hiscox.** 2006. Cell cycle perturbations induced by infection with the coronavirus infectious bronchitis virus and their effect on virus replication. J. Virol. **80:**4147–4156.
16. **Dveksler, G. S., C. W. Dieffenbach, C. B. Cardellichio, K. McCuaig, M. N. Pensiero, G. S. Jiang, N. Beauchemin, and K. V. Holmes.** 1993. Several members of the mouse carcinoembryonic antigen-related glycoprotein family are functional receptors for the coronavirus mouse hepatitis virus-A59. J. Virol. **67:**1–8.
17. **Emery, S. L., D. D. Erdman, M. D. Bowen, B. R. Newton, J. M. Winchell, R. F. Meyer, S. Tong, B. T. Cook, B. P. Holloway, K. A. McCaustland, P. A. Rota, B. Bankamp, L. E. Lowe, T. G. Ksiazek, W. J. Bellini, and L. J. Anderson.** 2004. Real-time reverse transcription-polymerase chain reaction assay for SARS-associated coronavirus. Emerg. Infect. Dis. **10:**311–316.
18. **Feng, L., Y. Xia, T. Yoshimura, and C. B. Wilson.** 1995. Modulation of neutrophil influx in glomerulonephritis in the rat with anti-macrophage inflammatory protein-2 (MIP-2) antibody. J. Clin. Investig. **95:**1009–1017.
19. **Fouchier, R. A., T. Kuiken, M. Schutten, G. van Amerongen, G. J. van Doornum, B. G. van den Hoogen, M. Peiris, W. Lim, K. Stohr, and A. D. Osterhaus.** 2003. Aetiology: Koch's postulates fulfilled for SARS virus. Nature **423:**240.
20. **Frana, M. F., J. N. Behnke, L. S. Sturman, and K. V. Holmes.** 1985. Proteolytic cleavage of the E2 glycoprotein of murine coronavirus: host-dependent differences in proteolytic cleavage and cell fusion. J. Virol. **56:**912–920.
21. **Fuerst, T. R., E. G. Niles, F. W. Studier, and B. Moss.** 1986. Eukaryotic transient-expression system based on recombinant vaccinia virus that synthesizes bacteriophage T7 RNA polymerase. Proc. Natl. Acad. Sci. USA **83:**8122–8126.
22. **Gargalovic, P. S., N. M. Gharavi, M. J. Clark, J. Pagnon, W. P. Yang, A. He, A. Truong, T. Baruch-Oren, J. A. Berliner, T. G. Kirchgessner, and A. J. Lusis.** 2006. The unfolded protein response is an important regulator of inflammatory genes in endothelial cells. Arterioscler. Thromb. Vasc. Biol. **26:**2490–2496.
23. **Gosert, R., A. Kanjanahaluethai, D. Egger, K. Bienz, and S. C. Baker.** 2002. RNA replication of mouse hepatitis virus takes place at double-membrane vesicles. J. Virol. **76:**3697–3708.
24. **Haskill, S., A. Peace, J. Morris, S. A. Sporn, A. Anisowicz, S. W. Lee, T. Smith, G. Martin, P. Ralph, and R. Sager.** 1990. Identification of three related human GRO genes encoding cytokine functions. Proc. Natl. Acad. Sci. USA **87:**7732–7736.
25. **He, B.** 2006. Viruses, endoplasmic reticulum stress, and interferon responses. Cell Death Differ. **13:**393–403.
26. **Hilton, A., L. Mizzen, G. MacIntyre, S. Cheley, and R. Anderson.** 1986. Translational control in murine hepatitis virus infection. J. Gen. Virol. **67:**923–932.
27. **Holmes, K. V., and J. N. Behnke.** 1981. Evolution of a coronavirus during persistent infection in vitro. Adv. Exp. Med. Biol. **142:**287–299.
28. **Hori, O., F. Ichinoda, A. Yamaguchi, T. Tamatani, M. Taniguchi, Y. Koyama, T. Katayama, M. Tohyama, D. M. Stern, K. Ozawa, Y. Kitao, and S. Ogawa.** 2004. Role of Herp in the endoplasmic reticulum stress response. Genes Cells **9:**457–469.
29. **Jacobs, L., W. J. Spaan, M. C. Horzinek, and B. A. Van der Zeijst.** 1981. Synthesis of subgenomic mRNA's of mouse hepatitis virus is initiated independently: evidence from UV transcription mapping. J. Virol. **39:**401–406.
30. **Koolen, M. J., A. D. Osterhaus, G. Van Steenis, M. C. Horzinek, and B. A. Van der Zeijst.** 1983. Temperature-sensitive mutants of mouse hepatitis virus strain A59: isolation, characterization and neuropathogenic properties. Virology **125:**393–402.
31. **Lamontagne, L. M., and J. M. Dupuy.** 1984. Persistent infection with mouse hepatitis virus 3 in mouse lymphoid cell lines. Infect. Immun. **44:**716–723.
32. **Lewicki, D. N., and T. M. Gallagher.** 2002. Quaternary structure of coronavirus spikes in complex with carcinoembryonic antigen-related cell adhesion molecule cellular receptors. J. Biol. Chem. **277:**19727–19734.
33. **Li, F., W. Li, M. Farzan, and S. C. Harrison.** 2005. Structure of SARS coronavirus spike receptor-binding domain complexed with receptor. Science **309:**1864–1868.
34. **Li, W., M. J. Moore, N. Vasilieva, J. Sui, S. K. Wong, M. A. Berne, M. Somasundaran, J. L. Sullivan, K. Luzuriaga, T. C. Greenough, H. Choe, and M. Farzan.** 2003. Angiotensin-converting enzyme 2 is a functional receptor for the SARS coronavirus. Nature **426:**450–454.
35. **Liang, S. H., W. Zhang, B. C. McGrath, P. Zhang, and D. R. Cavener.** 2006. PERK (eIF2α kinase) is required to activate the stress-activated MAPKs and induce the expression of immediate-early genes upon disruption of ER calcium homoeostasis. Biochem. J. **393:**201–209.
36. **Liu, Y., Y. Cai, and X. Zhang.** 2003. Induction of caspase-dependent apoptosis in cultured rat oligodendrocytes by murine coronavirus is mediated during cell entry and does not require virus replication. J. Virol. **77:**11952–11963.
37. **Luytjes, W., H. Gerritsma, E. Bos, and W. Spaan.** 1997. Characterization of two temperature-sensitive mutants of coronavirus mouse hepatitis virus strain A59 with maturation defects in the spike protein. J. Virol. **71:**949–955.
38. **Ma, Y., and L. M. Hendershot.** 2004. Herp is dually regulated by both the endoplasmic reticulum stress-specific branch of the unfolded protein response and a branch that is shared with other cellular stress pathways. J. Biol. Chem. **279:**13792–13799.
39. **Meyer, M., W. H. Caselmann, V. Schluter, R. Schreck, P. H. Hofschneider, and P. A. Baeuerle.** 1992. Hepatitis B virus transactivator MHBst: activation of NF-κB, selective inhibition by antioxidants and integral membrane localization. EMBO J. **11:**2991–3001.
40. **Miller, D. K., and J. Lenard.** 1982. Ultraviolet-irradiated vesicular stomatitis

virus and defective-interfering particles are similar non-specific inhibitors of virus infection. J. Gen. Virol. **60:**327–333.
41. **Mizutani, T., S. Fukushi, M. Saijo, I. Kurane, and S. Morikawa.** 2004. Phosphorylation of p38 MAPK and its downstream targets in SARS coronavirus-infected cells. Biochem. Biophys. Res. Commun. **319:**1228–1234.
42. **Opstelten, D. J., P. de Groote, M. C. Horzinek, H. Vennema, and P. J. Rottier.** 1993. Disulfide bonds in folding and transport of mouse hepatitis coronavirus glycoproteins. J. Virol. **67:**7394–7401.
43. **Pahl, H. L., and P. A. Baeuerle.** 1995. Expression of influenza virus hemagglutinin activates transcription factor NF-κB. J. Virol. **69:**1480–1484.
44. **Pahl, H. L., M. Sester, H. G. Burgert, and P. A. Baeuerle.** 1996. Activation of transcription factor NF-κB by the adenovirus E3/19K protein requires its ER retention. J. Cell Biol. **132:**511–522.
45. **Porter, F. W., Y. A. Bochkov, A. J. Albee, C. Wiese, and A. C. Palmenberg.** 2006. A picornavirus protein interacts with Ran-GTPase and disrupts nucleocytoplasmic transport. Proc. Natl. Acad. Sci. USA **103:**12417–12422.
46. **Rempel, J. D., S. J. Murray, J. Meisner, and M. J. Buchmeier.** 2004. Differential regulation of innate and adaptive immune responses in viral encephalitis. Virology **318:**381–392.
47. **Rempel, J. D., S. J. Murray, J. Meisner, and M. J. Buchmeier.** 2004. Mouse hepatitis virus neurovirulence: evidence of a linkage between S glycoprotein expression and immunopathology. Virology **318:**45–54.
48. **Rottier, P. J., W. J. Spaan, M. C. Horzinek, and B. A. Van der Zeijst.** 1981. Translation of three mouse hepatitis virus strain A59 subgenomic RNAs in *Xenopus laevis* oocytes. J. Virol. **38:**20–26.
49. **Schröder, M., and R. J. Kaufman.** 2005. The mammalian unfolded protein response. Annu. Rev. Biochem. **74:**739–789.
50. **Schulze, A., S. Standera, E. Buerger, M. Kikkert, S. van Voorden, E. Wiertz, F. Koning, P. M. Kloetzel, and M. Seeger.** 2005. The ubiquitin-domain protein HERP forms a complex with components of the endoplasmic reticulum associated degradation pathway. J. Mol. Biol. **354:**1021–1027.
51. **Snijder, E. J., P. J. Bredenbeek, J. C. Dobbe, V. Thiel, J. Ziebuhr, L. L. Poon, Y. Guan, M. Rozanov, W. J. Spaan, and A. E. Gorbalenya.** 2003. Unique and conserved features of genome and proteome of SARS-coronavirus, an early split-off from the coronavirus group 2 lineage. J. Mol. Biol. **331:**991–1004.
52. **Snijder, E. J., Y. van der Meer, J. Zevenhoven-Dobbe, J. J. Onderwater, J. van der Meulen, H. K. Koerten, and A. M. Mommaas.** 2006. Ultrastructure and origin of membrane vesicles associated with the severe acute respiratory syndrome coronavirus replication complex. J. Virol. **80:**5927–5940.
53. **Su, H. L., C. L. Liao, and Y. L. Lin.** 2002. Japanese encephalitis virus infection initiates endoplasmic reticulum stress and an unfolded protein response. J. Virol. **76:**4162–4171.
54. **Tekamp-Olson, P., C. Gallegos, D. Bauer, J. McClain, B. Sherry, M. Fabre, S. van Deventer, and A. Cerami.** 1990. Cloning and characterization of cDNAs for murine macrophage inflammatory protein 2 and its human homologues. J. Exp. Med. **172:**911–919.
55. **Vennema, H., L. Heijnen, A. Zijderveld, M. C. Horzinek, and W. J. Spaan.** 1990. Intracellular transport of recombinant coronavirus spike proteins: implications for virus assembly. J. Virol. **64:**339–346.
56. **Vennema, H., R. Rijnbrand, L. Heijnen, M. C. Horzinek, and W. J. Spaan.** 1991. Enhancement of the vaccinia virus/phage T7 RNA polymerase expression system using encephalomyocarditis virus 5′-untranslated region sequences. Gene **108:**201–209.
57. **Versteeg, G. A., P. J. Bredenbeek, S. H. van den Worm, and W. J. Spaan.** 2007. Group 2 coronaviruses prevent immediate early interferon induction by protection of viral RNA from host cell recognition. Virology **361:**18–26.
58. **Versteeg, G. A., O. Slobodskaya, and W. J. Spaan.** 2006. Transcriptional profiling of acute cytopathic murine hepatitis virus infection in fibroblast-like cells. J. Gen. Virol. **87:**1961–1975.
59. **Watowich, S. S., R. I. Morimoto, and R. A. Lamb.** 1991. Flux of the paramyxovirus hemagglutinin-neuraminidase glycoprotein through the endoplasmic reticulum activates transcription of the GRP78-BiP gene. J. Virol. **65:**3590–3597.
60. **Yoshida, H., T. Matsui, A. Yamamoto, T. Okada, and K. Mori.** 2001. XBP1 mRNA is induced by ATF6 and spliced by IRE1 in response to ER stress to produce a highly active transcription factor. Cell **107:**881–891.
61. **Zhang, K., X. Shen, J. Wu, K. Sakaki, T. Saunders, D. T. Rutkowski, S. H. Back, and R. J. Kaufman.** 2006. Endoplasmic reticulum stress activates cleavage of CREBH to induce a systemic inflammatory response. Cell **124:**587–599.
62. **Zheng, Y., B. Gao, L. Ye, L. Kong, W. Jing, X. Yang, Z. Wu, and L. Ye.** 2005. Hepatitis C virus non-structural protein NS4B can modulate an unfolded protein response. J. Microbiol. **43:**529–536.